The Development of an Active Magnetic Regenerative Refrigerator (AMRR) for Sub-Kelvin Cooling of Space Science Instrumentation

C. M. Gunderson, G. F. Nellis, F. K. Miller

University of Wisconsin-Madison
Madison, WI 53715

ABSTRACT

Sub-Kelvin operating temperatures are required for a wide range of space science instrumentation. Consistent and reliable cooling of these instruments is critical to ensure adequate performance in high sensitivity applications. This research works towards the development of a sub-Kelvin Active Magnetic Regenerative Refrigeration (AMRR) system that can provide an estimated 600 μW of distributed cooling at 900 mK to space instrumentation via circulation of a ^{3}He-^{4}He mixture. The AMRR uses a Superfluid Magnetic Pump (SMP) to circulate superfluid ^{3}He-^{4}He mixture throughout the rest of the system, which consists of two hot heat exchangers, one cold heat exchanger, and two magnetic regenerators. This paper provides a brief overview of the system and discusses the design and fabrication of the AMRR regenerator components in detail.

INTRODUCTION

Cryogenic detectors have higher sensitivity and better energy resolution than alternative sensors, making them an attractive option for space exploration and essential for observing low energy photons in the near- or far-IR, X-ray, and submillimeter ranges[1]. Since NASA's first cryogenic missions in the early 1980s, increasingly complex space detectors have required continuous advancement in cryogenic technology[2]. Existing solutions are not ideal, especially when approaching sub-Kelvin temperatures, and advances in these refrigeration technologies would have widespread impact as many high sensitivity applications in current and future NASA missions rely on cryogenic temperatures for operation.

^{3}He evaporation refrigerators and Adiabatic Demagnetization Refrigerators (ADRs) are presently used to provide sub-Kelvin cooling, but substantial amounts of magnetic shielding for ADRs are needed to protect the instrument due to the need for close proximity between the detector and magnets. This distance cannot easily be increased because of the requirement for a highly conductive thermal link between the ADR system and the detector. The heat switches that are required throughout the remainder of the ADR system introduce additional inefficiencies, locations for possible failure, and weight into the system. Consequently, the system is heavier and less reliable than is desired – both important considerations for space technology. Additionally, scaling this system to increase cooling power will substantially increase mass as the heaviest components involved, such as the shielding and the thermal links, tend to scale similarly. Increased efficiency and reliability related to cooling state-of-the-art, low-noise detectors and optics would enable scientists to improve the

Cryocoolers 21, edited by R.G. Ross, Jr., J.R. Raab and S.D. Miller

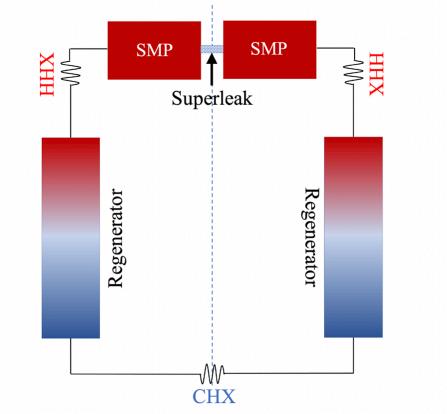

Figure 1. A diagram of the AMRR system.

resolution and range of data collection both in space and on the ground, allowing NASA to continue to push the bounds of human knowledge through discovery.

The development of a sub-Kelvin Active Magnetic Regenerative Refrigerator (AMRR) is discussed in this work. The initial proof-of-concept system will provide cooling down to approximately 900 mK with a predicted cooling power of 600 μW – 1 mW, though future iterations with different types of magnetic refrigerant could reduce the cold end temperature. This novel AMRR addresses many of the deficiencies of current cooling solutions as it can provide continuous and distributed sub-Kelvin cooling via circulation of a ^{3}He-^{4}He mixture using a non-moving Superfluid Magnetic Pump (SMP). The resulting system eliminates the requirement for heat switches, extends the allowable distance between the detector and magnets, and is a reliable, no-vibration, low mass, and scalable sub-Kelvin cooling solution for space instrumentation. Additionally, the system provides distributed cooling which enables a variety of thermal integration options. For example, the refrigeration of large areas and detector arrays or integration via microchannels within detectors are all possible; this is a significant advantage over other cryogenic refrigeration options.

A SMP, two regenerators, one cold heat exchanger, and two hot heat exchangers comprise the AMRR system shown in Figure 1. The left-hand side (LHS) and right-hand side (RHS) operate identically and 180° out of phase of each other. This is a novel AMRR in that it uses the nearly thermodynamically reversible SMP to displace the fluid, resulting in a system with no moving parts. This greatly increases the reliability of the system and makes it a strong candidate for use in space cooling sensitive instruments.

The ultimate goal of this research is to design and construct a complete proof-of-concept AMRR system to show that it is a viable option for cryogenic cooling of space instrumentation. A simple numerical model of the system was created for use as a design tool to size the components required by the system. Many of the SMP components were already available so the bulk of the work was focused on the design and fabrication of the remaining AMRR components. For a detailed explanation of the theory and design of the SMP, see Jahromi[3]. Future work includes completing the AMRR assembly and experimentally validating the system.

BACKGROUND

In order to provide distributed sub-Kelvin cooling, the AMRR system takes advantage of a few key characteristics of both the paramagnetic refrigerant and the helium working fluid mixture. The unique combination of these properties enables the refrigeration cycle as well as oscillatory flow provided with a non-moving pump.

GGG and the Magnetocaloric Effect

The remarkable qualities of paramagnetic materials make ultra-low temperature refrigeration possible. Paramagnetic materials have magnetic properties due to unfilled electron shells in some of the ions which create magnetic moments and result in a total electronic angular momentum (J)[4].

When the material is placed in an external field, these moments will align with the applied field and reduce the magnetic entropy in the material. Consequently, the thermal entropy and temperature increase, maintaining constant total entropy in the system. This exchange, known as the magnetocaloric effect[4,5], occurs between the adiabatic and isothermal limits, depending on the rate at which heat is removed from the system. Manipulation of this coupling allows for the heating or cooling of paramagnetic material through the magnetization or demagnetization of an applied field, respectively, and is the primary motivation behind using these materials in refrigeration. The paramagnetic refrigerant used in this research, Gadolinium Gallium Garnet (GGG), is typically used in the temperature range from approximately 1 K up to 20 K, although the magnetocaloric effect diminishes approaching the upper temperature limit[4].

^{3}He-^{4}He Mixture Properties

Helium is the only element that is liquid in the operating temperature range of the AMRR, making it the sole option for the system working fluid. At near and sub-Kelvin temperatures, each of the two stable helium isotopes exhibits unique properties. When combined, these individual properties, as well as interaction effects between the isotopes, contribute to the overall suitability of the mixture for the AMRR system.

Helium has two protons, two electrons, and one or two neutrons (for ^{3}He and ^{4}He, respectively). ^{3}He has a total nuclear spin of ½ due to this unmatched neutron, and therefore obeys Fermi-Dirac statistics resulting in its unusual low temperature properties[6]. ^{4}He, on the other hand, has net zero nuclear spin and obeys Bose-Einstein statistics, allowing for Bose-Einstein condensation[7]. Below the Bose-Einstein condensation temperature (T_C), an increasing fraction of bosons occupy – or "condense into" – the lowest energy state[7]. In ^{4}He, this transition point is known as the λ-line and occurs around 2.17 K[7]. When the temperature is reduced to approximately 1 K, 99% of the ^{4}He has transitioned into a superfluid, which has no viscosity and no entropy[7]. The ^{4}He phases at temperatures above and below this λ transition have markedly different properties and are called He I and He II, respectively[7]. The most important difference for the AMRR cycle is the significant reduction in heat capacity below the λ temperature, as the superfluid state cannot carry energy. This is in contrast to ^{3}He, whose large magnetic spin entropy gives rise to a large heat capacity, 40 times larger than the heat capacity of ^{4}He at 1 K[7]. Consequently, ^{3}He is required to carry energy throughout the system. Though He II cannot carry energy, it still plays a significant role in the mixture as it is responsible for driving flow in the system through the thermomechanical fountain effect[7,8]. Essentially, if two bodies of He II are separated by a superleak plug (through which only the superfluid portion can flow), the superfluid will cross between the bodies to maintain a constant chemical potential between both systems. If one body is heated, a portion of the superfluid is promoted into its normal state and the chemical potential is reduced. This reduction results in an influx of superfluid from the cooler body that is driven to find a new equilibrium. The incoming superfluid displaces a portion of the mixture, "fountaining" it out of the respective body. When both isotopes are combined in the mixture, the ^{3}He is viscously interlocked with the normal ^{4}He portion of He II and is thus expelled with the displaced fluid, creating flow in the system.

The AMRR system therefore requires a mixture of both isotopes, capitalizing on the individual properties of both ^{3}He and ^{4}He, and the way they interact as a mixture. In order to model the AMRR system, thermodynamic ^{3}He-^{4}He mixture properties are taken from Chaudhry[9], who fit property curves to smoothed data sets for ^{3}He-^{4}He mixtures.

AMRR System Operation

The AMRR system utilizes both GGG and helium mixture properties to provide distributed cryogenic refrigeration. The SMP is composed of two separate canisters that are each filled with finely crushed GGG particles. The canisters are suspended within the bores of superconducting magnets. A superleak with 4 nm pores connects the two pump canisters and allows superfluid ^{4}He to move freely between the two beds. To produce flow, the current in one coil is increased while the current in the opposite coil is decreased, resulting in increasing and decreasing magnetic fields, respectively. The shift in applied fields causes the thermal and magnetic entropies in the paramagnetic beds to also change due to the previously explained magnetocaloric effect. As the magnetic field in one canister

rises, the magnetic entropy of the GGG must decrease. The thermal entropy thus increases, offsetting the magnetic change to the total entropy and raising the overall temperature. Because the ^{3}He-^{4}He is in good thermal contact with the GGG, the fluid tracks the temperature of the particles very closely. The increase in temperature promotes a portion of the ^{4}He from the superfluid state to the normal state, and forces fluid to exit the canister through the normal port into the rest of the system. The opposite is true for the canister experiencing a decreasing magnetic field. The superleak maintains continuity in the system, allowing only superfluid ^{4}He to cross from the cooling canister into the warming canister to replace the promoted ^{4}He and maintain a constant chemical potential. Flow in the system is reversed by alternating between increasing and decreasing the magnetic fields in each canister.

The magnetic regenerators are almost identical to the pump in construction. Canisters of crushed paramagnetic GGG are suspended inside the bore of superconducting solenoids by Kevlar strands. As fluid is forced out through the warming pump bed, it moves down through the demagnetizing regenerator, which cools the mixture so that it exits the regenerator bed at the desired outlet temperature. The mixture then moves through a cold heat exchanger (CHX), providing sub-Kelvin cooling to the load (e.g., one or more detectors). It flows back up through the opposite, magnetizing regenerator which rejects more heat into the fluid. Finally, this heat is rejected to the precooling stage at a temperature of approximately 1.6 K. The system can then be reversed, sending flow back in the opposite direction. One full cycle consists of an 80 second clockwise flow process, a 10 second no-flow process, an 80 second counterclockwise flow process, and a 10 second no-flow process. During the no-flow processes, the regenerators change field to adjust their cold-end temperatures and prepare for flow in the opposite direction. The fact that this system produces a flow is one of the most important advantages associated with the AMRR relative to other cryogenic refrigeration solutions.

AMRR SYSTEM DESIGN

As stated previously, the primary objective of this research is to provide measurable cooling at the CHX with a proof-of-concept, novel AMRR. This relies on appropriately designing the remaining system components relative to the existing SMP to ensure that there is enough paramagnetic material and sufficient magnetic field to force circulation and lift heat at the CHX.

Regenerator Design Model

Our simplified 1D transient design model focused on one regenerator canister during a flow process in the AMRR system. The control volume (CV) for the regenerator is indicated by the dashed box in Figure 2 and contains only the fluid; the mixture enters at the left from the HHX at 1.6 K and exits on the right to the CHX at 750 mK. We assume a constant linear temperature distribution between these two extremes across the regenerator; this conservatively implies no internal energy change. The GGG particles are represented by the black box below the CV, and the magnetocaloric effect is captured through the heat exchange between the fluid and particles at the CV boundary according to the second law balance:

$$\frac{dQ_{GGG}}{T} = dS_{GGG}(B,T), \tag{1}$$

where dQ_{GGG} is the heat into the GGG, dS_{GGG} is the entropy change of the GGG, and T is the temperature at the boundary. The GGG is discretized into spatial (i=1…N) and temporal (j=1…M) nodes. This captures the entropy dependence on changing magnetic field and the spatial variation in local temperature. Rearranging terms and expanding the expression for entropy provides the total heat into the GGG in node i during timestep j:

$$Q_{GGG,i,j} = T_i \cdot n_{GGG}\left(\left.\frac{\partial s}{\partial B}\right|_{B=B_j}\left(B_{j+1} - B_j\right)\right), \tag{2}$$

where T_i is the boundary temperature at node i, n_{GGG} is the number of moles of GGG in node i, B_j is the field at time j, and the derivative of the entropy as a function of magnetic field is evaluated at B_j. Note that we can ignore temperature-driven changes in the entropy as we are assuming a constant (in time) temperature throughout the process. Summing over i from 1 to N sums the heat contributions from every node and summing over j from 1 to M sums the heat contributions over the entire process.

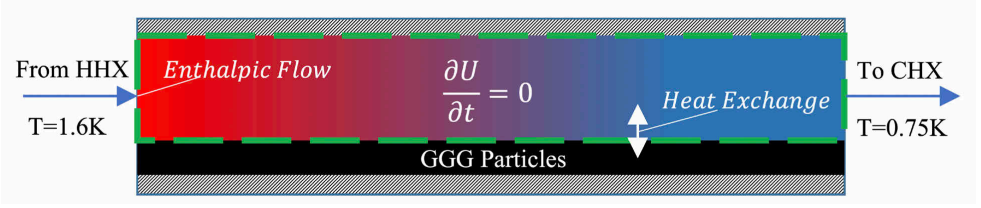

Figure 2. Control volume for regenerator canister. Fluid enters from the HHX at the left and exits to the CHX on the right.

Performing a first law energy balance on the total CV gives:

$$n_{in}h_{flow,HHX} = n_{out}h_{flow,CHX} + \sum_{j=1}^{M}\sum_{i=1}^{N} Q_{GGG,i,j}, \quad (3)$$

where n_{in} and n_{out} are the number of moles of mixture moving into or out of the regenerator, respectively, $h_{flow,HHX}$ and $h_{flow,CHX}$ are the molar specific enthalpies of the mixture at the two ends of the regenerator and $Q_{GGG,i,j}$ is, again, the heat out of the mixture into the GGG.

The design constraints included the inner diameter of our canister, the maximum allowable field swing, which determined our field values used in our entropy calculation, and the total number of moles circulated through the regenerator, which determined our enthalpy term. Using Eq. (3), we were able to determine the canister length required to maintain an outlet temperature of 750 mK during the flow process.

The final regenerator canister dimensions and required field swing are then used to constrain the magnet design. The equation for the magnetic field along the axis of a solenoid is derived in Jahromi[3], and is given as:

$$B_{axis,inside} = \frac{\mu_0 N_{turn} I}{2}\left[\frac{x}{\sqrt{x^2+R_{coil}^2}} + \frac{L_{coil}-x}{\sqrt{(L_{coil}-x)^2+R_{coil}^2}}\right], \quad (4)$$

where u_0 is the permeability of free space, $4\pi\times10^{-7}$ (N/A^2), N_{turn} is the total turns per unit length, I is the current in the coil, x is the axial location, L_{coil} is the length of the coil, and R_{coil} is the effective radius of the coil, calculated at half of the coil thickness. This equation can be used to find the total number of turns for a given mandrel geometry required to reach the desired field at the center of the coil. For the regenerator, the magnets were designed to reach a maximum of 1.5 T, more than twice the required field for the flow process according to the simple model.

FINAL COMPONENT DESIGNS

Using both the simplified regenerator model and magnet design code, the remaining AMRR components were designed. The final regenerator design includes the canister pieces, magnet mandrel and winding specifications, and suspension system for thermally isolating and centering the canister within the bore of the magnet. The final design is shown in Figure 3.

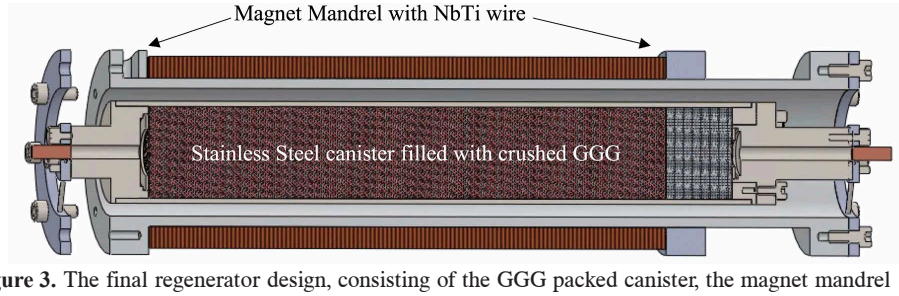

Figure 3. The final regenerator design, consisting of the GGG packed canister, the magnet mandrel and windings, and the suspension components.

Table 1. Key parameters of the final regenerator magnet and canister designs.

Regenerator Canister		Regenerator Magnet	
Canister Material	304 Stainless Steel	Mandrel Material	6061 Aluminum
ID [m]	0.0229 m	ID [m]	0.03175 m
OD [m]	0.0254 m	OD [m]	0.0508 m
Porosity [-]	0.38	Coil Material	54S43 NbTi
GGG Fill Length [m]	0.133 m	Coil Length [m]	0.133 m
Glass Fill Length [m]	0.017 m	Current [A]	4.7 A
Total Mass GGG [kg]	0.240 kg	Number of Turns [-]	37,000
Total Mass Canister [kg]	0.204 kg	Max Field [T]	1.5 T

The regenerator canister is composed of four stainless steel pieces: thin-walled tube and three end caps. Two of these end caps are welded to the tube, one with an opening to allow for packing, and the third is sealed into the open cap with indium after the canister is packed with GGG. Inlet and outlet headers are included in the endcaps to allow for even flow distribution radially across the regenerator. Fine mesh screens are used to prevent the movement of GGG particles into these volumes, consequently preventing the displacement of GGG into the remainder of the system.

The regenerator magnet consists of a niobium-titanium (NbTi) coil potted on an aluminum mandrel. The wire chosen contains 54 NbTi filaments, each with a diameter of 9 μm, embedded in a stabilizing copper matrix with a total insulated diameter of 0.127 mm. This diameter, along with a conservative current of 4.7 A, was used to determine the number of turns required to reach 1.5 T in the center of a magnet.

The final regenerator component, the suspension, is composed of a center disk suspended by Kevlar within a thin aluminum ring. The center disk attaches to the regenerator canister, while the outer ring is supported by the magnet mandrel, centering the canister within the bore of the magnet. Kevlar is very strong in tension, having a tensile strength around 2.5 GPa, and also has a very low thermal conductivity. These qualities make it an attractive option for use in suspending and thermally isolating the canister. A summary of key final regenerator design parameters is provided in Table 1.

COMPONENT CONSTRUCTION AND SYSTEM ASSEMBLY

Following the finalization of design, we constructed the remaining AMRR components. This primarily included machining the canister, mandrel, and suspension components, winding the magnets, and crushing and packing the GGG into the canisters.

Regenerator Canisters

As previously mentioned, the canister assembly consists of one thin-walled tube and three endcaps, all machined out of stainless steel. Two of the endcaps are shown in Figure 4. The endcap on the left is welded to the end of the tube to provide a sealing surface once the GGG has been packed. This cap has a large through hole to both allow for packing and create a header volume for better distribution of incoming fluid. The endcap on the right screws into the one on the left, pulling down on the indium ring between the two pieces to prevent leaks. Two mesh screens are fit into the header volume to prevent GGG particles from escaping. The third endcap is similar to the one on the right, in that it has a header volume blocked by screens, but it does not have through holes and is simply welded onto the opposite side of the canister. One complete regenerator is shown in Figure 5. Brazed into each outermost endcap is a short length of copper tubing to allow for easy integration with the rest of the system assembly.

Though GGG crushes into irregular shapes, the target particle size was roughly 1 mm in diameter. To achieve this, two sieves with 1.2 mm and 0.2 mm hole widths were used to create a go no-go gage. Figure 6 shows an image of the sieves taken during the crushing process. Large chunks of the crystal were hammered into finer pieces, which were placed on top of the wider sieve and shaken to ensure that all particles with diameter <1.2 mm would pass through into the second sieve.

Figure 4. An example of two of the three canister endcaps.

Figure 5. One finished regenerator canister.

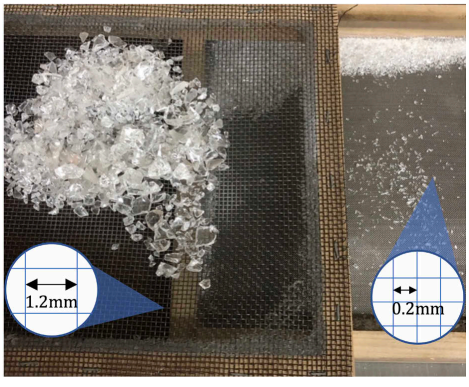

Figure 6. The two sieves used to achieve a GGG particle size of approximately 1 mm.

The particles collected in the second sieve could be used to pack the canister beds. Any finer particles that passed through the second sieve were discarded.In order to realize the optimal porosity of 0.38 in the canisters, we determined the mass of GGG required to fill 62% of the internal canister volume. We slowly packed this mass into the canister, vibrating the canister throughout the process to ensure even distribution of the particles. Once filled, we screwed on the canister end caps and vibrated the canister to allow the particles to settle further. We then reopened the canister to fill the small void created from settling and repeated this void filling process until there was no void from settling to guarantee that the particles were packed tightly and would not shift during operation.

Regenerator Magnets

We used thick walled 6061 Aluminum tubing to create the magnet mandrels, turning down the outer radius to form flanges on either side of the winding length and reach the required mandrel thickness. An additional collar was installed in order to modify the magnet wind length based on the allowable traverse of the winder; epoxy was used to create a smooth and continuous surface around the face of the collar.

To prepare for winding, we polished the winding surface and flanges using 6 different 3M polishing papers, which stepped down from 30-micron paper to 1-micron paper. Polishing the mandrel is crucial because under the forces created by the winding process and the magnetic fields even small imperfections on the surface could cut through the wire insulation and short the coil to the mandrel. Once polished, the surface was extensively cleaned to remove any paper fibers or residue from machining. We subsequently wrapped the winding surface and flanges using 0.025 mm thick Kapton to further protect against shorts by creating a backup insulation layer between the coil and mandrel. The Kapton layer also minimally increases the thermal resistance between the coil and mandrel, an important consideration in the event of a quench when the coil must reject heat to the mandrel.

Prior to winding, the wire is wrapped and secured around one of the flanges to provide an adequate lead length. The wire is fed through the diode pocket into the mandrel and secured at the entry point. Care is taken not to wrap the wire tightly around one edge of the channel when entering the winding surface. A picture of this setup is shown in Figure 7.

During the winding process, we continuously brushed CTD-A521 magnet epoxy onto the coil using a silicone bristle brush. Potting the coil in epoxy helps prevent frictional heating in the magnet by preventing movement of the coil loops due to forces created during magnetization. The epoxy also helps to create good thermal contact between the wires and mandrel, allowing for efficient heat rejection.

Once the number of required turns was reached, we wrapped and fastened the second magnet lead around the flange. In order to prevent the epoxy from running off or distorting the coil, the magnet was slowly rotated on the winding machine for at least 24 hours as the epoxy cured. Images of the

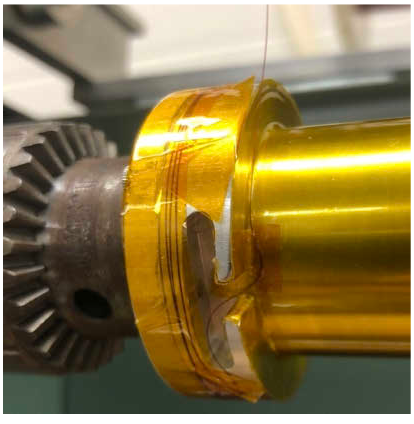

Figure 7. The setup of one magnet mandrel prior to winding.

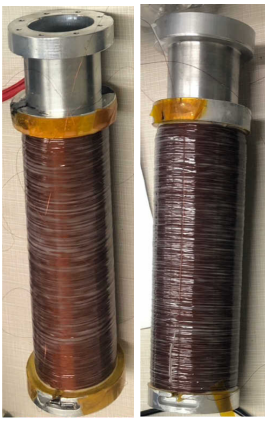

Figure 8. The two regenerator magnets.

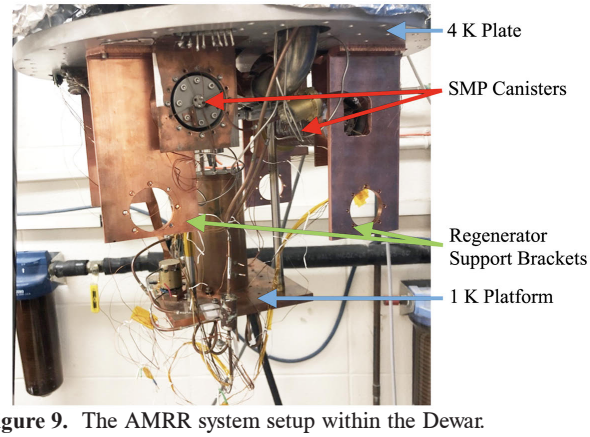

Figure 9. The AMRR system setup within the Dewar.

magnets following the winding process are shown in Figure 8. To finish the magnets, we stripped the insulation on the leads in the diode pocket, and then soldered two back-to-back 1N4001 diodes across the leads. This pocket is then filled with epoxy to secure the diode configuration and create a good thermal link to the mandrel. As noted previously, the current is redirected through these diodes in the event of a quench, when the voltage across the coil leads exceeds the forward voltage of the diodes. The diodes are placed back-to-back so that the direction of the applied current does not matter.

AMRR Assembly

The physical AMRR configuration is shown in Figure 9. As shown, the regenerator brackets are positioned to align the regenerators parallel to and approximately below the SMP canisters. The circulation path will be configured so that while one regenerator is magnetizing, the above pump canister is also magnetizing and vice versa so as to minimize deconstructive interference with the magnetic fields.

The HHXs that will be used in the AMRR system are already integrated into the Dewar and are attached to the bottom of the 1 K stage. The temperature of this platform can be controlled by a heater to maintain a precooling temperature around 1.6 K. The CHX consists of tubing attached to a copper plate with a heater to allow for control and measurement of the cooling power of the system. This heat exchanger will be suspended from the bottom of the 1 K plate to thermally isolate it and minimize parasitic loads.

Several of the regenerator components have been installed, and thus the remaining work to finish the AMRR system assembly consists primarily of integrating the components with a circulation loop.

CONCLUSION AND FUTURE WORK

This work focused on the design and development of a complete proof-of-concept AMRR system using GGG as the refrigerant with a ^{3}He-^{4}He working fluid. Though the utilization of the magnetocaloric effect for low temperature refrigeration is not novel, the combination of this technique with the SMP in order to provide distributed sub-Kelvin cooling with no moving parts is truly unique. Once optimized, this system can be used to provide precooling to even lower temperature stages or for distributed cooling over large areas, offering an improvement over current systems and making new types of cryogenic refrigeration configurations possible.

The SMP used to create circulation within the AMRR system has already been developed and tested at UW-Madison. The remaining components, i.e. the heat exchangers and regenerators, were designed to be consistent with this existing pump and provide measurable cooling at the cold end. The two regenerator magnets were designed to reach fields of 1.5 T, more than twice the predicted required field determined using the simple thermodynamic system model in order to account for unforeseen challenges and modeling assumptions. Each regenerator canister was filled with GGG particles approximately 1 mm or less in diameter to a design porosity of 0.38 and then sealed through welding, brazing, and indium rings. The regenerator canisters were then suspended within the magnets to complete the construction of the regenerators.

Near-term future work includes finishing the assembly of and experimentally validating the AMRR system. Once the AMRR developed in this work has been experimentally tested, we intend to redesign the system using GLF as the paramagnetic regenerator refrigerant, which will allow the system to reach temperatures as low as 0.35 K, substantially lowering the cold end temperature. The insights gained from the GGG design will allow for a more optimal design and a more thorough understanding of the operating space of the system.

Finally, the development of a comprehensive AMRR numerical model would be useful in future system design and optimization, especially for advancing the system technology towards providing reliable cooling for space-flight applications. The data from the GGG and GLF AMRR systems can be used to experimentally validate this model.

ACKNOWLEDGMENT

This work was supported by a NASA Space Technology Research Fellowship.

REFERENCES

1. Rando, N., Lumb, D., Bavdaz, M., Martin, D., and Peacock, T., "Space science applications of cryogenic detectors," *Nuclear Instruments and Methods in Physics Research Section A: Accelerators, Spectrometers, Detectors and Associated Equipment*, Vol. 522, No. 1-2 (2004), pp. 62-68.
2. Rando, N., "Cryogenics in Space," *Observing Photons in Space*, ISSI Scientific Report Series, Vol. 9, Springer, New York (2013), pp. 639-655.
3. Jahromi, A.E., "*Development of a Proof of Concept Low Temperature Superfluid Magnetic Pump with Applications*," PhD dissertation at University of Wisconsin-Madison (2015).
4. Wikus, P., Canavan, E., Heine, S.T., Matsumoto, K., and Numazawa, T., "Magnetocaloric Materials and the Optimization of Cooling Power Density," *Cryogenics,* Vol. 62, (2014), pp. 150-162.
5. Pecharsky, V.K. and Gschneider Jr., K.A., "Magnetocaloric effect and magnetic refrigeration," *Journal of Magnetism and Magnetic Materials*, Vol. 200, (1999), pp. 44-56.
6. Wolfle, P. and Vollhardt, D., *The Superfluid Phases of Helium 3*, Dover Publications, Inc., Mineola (1990).
7. Sciver, S. V., *Helium Cryogenics*, Springer, New York (2012).
8. Papoular, D.J., Ferrari, G., Pitaevskii, L.P., and Stringari, S., "Increasing Quantum Degeneracy by Heating a Superfluid," *Physical Review Letters,* Vol. 109, No. 8-24 (2012).
9. G. Chaudhry, "*Thermodynamic properties of liquid ^{3}He-^{4}He mixtures between 0.15 K and 1.8 K*," PhD dissertation at Massachusetts Institute of Technology (2009).